Generic VSC-Based DC Grid EMT Modeling, Simulation, and Validation on a Scaled Hardware Platform

Luigi Vanfretti[1,2], Wei Li[1], Agustí Egea-Alvarez[3], and Oriol Gomis-Bellmunt[3,4]

[1]School of Electrical Engineering, KTH Royal Institute of Technology, Stockholm, Sweden
[2]Statnett SF, R&D, Oslo, Norway
[3]CITCEA, UPC Universitat Politècnica de Catalunya, Barcelona, Spain
[4]IREC Catalonia Institute for Energy Research, Barcelona, Spain

***Abstract*—This paper presents results from the KIC InnoEnergy project: Generic DC grid off-line and real-time simulation models and tools (Action 2.1, Subtask 2.1.1). The work reported here is focused on the development of a generic voltage source converter (VSC) model and its control schemes. Different test systems were designed and implemented in simulation tools and an experimental platform to verify the proposed generic model. Consistent simulation and emulation performances indicate that the generic model and its control schemes are applicable for VSC-HVDC operation, and thus, they can facilitate further research and development in DC grids.**

I. Introduction

In the last 20 years, the importance of high voltage direct current (HVDC) long distance interconnections and back-to-back couplings has significantly increased all over the world. Even though the application of point-to-point HVDC links is well known, there are plentiful open questions for the operation of HVDC links within a meshed grid. Unfortunately, detailed DC grid models using realistic data are not available for research due to commercial and trade secret reasons. To overcome this drawback, the work presented in this paper developed generic voltage source converter (VSC) model, its control schemes, and DC grid test systems. To assess the validity and applicability of these models, a scale-down hardware-based platform was used for validation of the models' response.

Within the KIC InnoEnergy project: Generic DC grid off-line and real-time simulation models and tools (Action 2.1 Subtask 2.1.1), KTH SmarTS Lab and UPC collaborated together for the model development and its validation . First, DC grid generic control models suitable for off-line and real-time simulations for electromagnetic transient (EMT) analysis were developed. This included a standard generic low-level control model and a new generic high-level control model. In order to examine the generic control models' performance, different test systems were developed, such as one terminal VSC station, point-to-point VSC-HVDC link, four-terminal VSC DC grid. Moreover, off-line and real-time simulations of these test systems were performed in KTH SmarTS Lab. Ultimately, validation tests were carried out in UPC by using a scale-down platform.

The remainder of this paper is organized as follows. Section II presents the generic VSC components and control models. Sequentially, different test systems are shown in Section III. Simulation tools and the validation platform are presented in Section IV. Section V presents simulation results and analyses, which are followed by the conclusion and discussion in Section VI.

II. Generic VSC-HVDC models and its control schemes

A. Generic VSC model

Figure 1 shows the main circuit diagram of a VSC converter. Point *P* is the point of common coupling (PCC), whose left side connects with an AC system through an AC transformer and right side with a VSC [1].

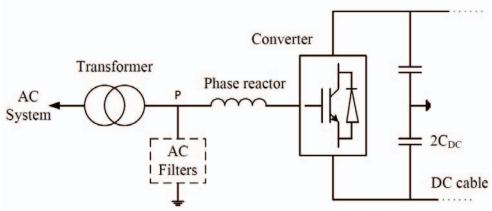

Fig. 1. The main circuit diagram of a VSC converter

The VSC model proposed in this work uses a three-phase two-level topology, which is the simplest and mostly used topology in VSC-HVDC technology. Each phase leg consists of two switches which are switched on or off to control the output voltage. Each switch comprises insulated-gate bipolar transistors (IGBTs) and anti-parallel diodes. This configuration suits bidirectional power flow. The midpoint of each phase leg connects to the output of three-phase AC lines.

The switching signal generation for IGBTs can be controlled by various schemes. In this project, the sinusoidal pulse width modulation (SPWM) method was used. In SPWM the reference waveform is compared with the carrier waveform to generate the switching signals for IGBTs [2]. If the reference waveform is greater than the carrier waveform, the upper IGBT of a phase leg will be turned on, i.e. $S_{(a-up)} = 1$. Otherwise, if the reference waveform is smaller than the carrier waveform, the lower IGBT of the same phase leg will be turned on, i.e. $S_{(a-low)} = 1$.

As shown in Fig. 1, an AC filter is adjacent to the PCC. This capacitor can suppress harmonics generated by SPWM

978-1-4673-8040-9/15/$31.00 ©2015 IEEE

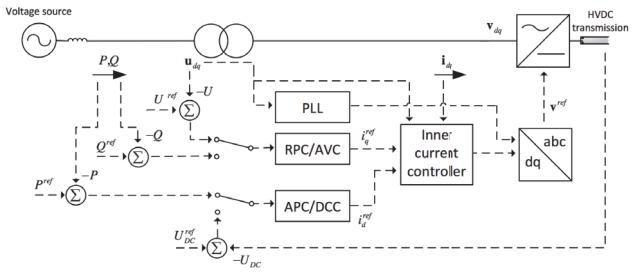

Fig. 2. Main circuit including the control block diagram for vector-current control. The blocks include the phase-locked loop (PLL), reactive-power controller (RPC), alternating-voltage controller (AVC), active-power controller (APC) and DC-controller (DCC). [6]

technique, thus avoiding the harmonics emitting into the AC system. Moreover, it can act as a reactive power source [2] [3]. The selection of the reactor value depends on the switching frequency. It is generally chosen between 0.15∼0.2 $p.u$ of the base impedance [4]. In this case, 0.15 $p.u.$ is selected.

The other component connecting to the PCC is a phase reactor. It operates as a low-pass filter to suppress the high-order harmonics generated by IGBT switching and assists to control active and reactive power by regulating the current flowing through it [2] [3]. In addition, it limits the short-circuit currents.

On the DC side, two capacitors are installed to suppress the harmonics in DC current generated by ripples in DC voltage due to the SPWM technique. The magnitude of voltage ripples depends on the DC capacitor size and switching frequency. In addition, the design of DC capacitors has to consider both steady state and transient dynamics, (see [2]).

B. Generic VSC control model

Generally, VSCs contain a two-level control scheme. The low-level control scheme, e.g. SPWM, regulates the switching signal generation and provides switching pulses for IGBT valves, as mentioned in Subsection II-A, by using the voltage references for each phase provided by high-level control scheme. The high-level control scheme, on the other hand, attempts to maintain the system DC voltage, active power, AC voltage and reactive power.

As mentioned in Subsection II-A, SPWM was chosen for the low-level control scheme. With respect to the high-level control scheme, vector-current control was used as it has been applied on many actual VSC-HVDC link installations. Furthermore, there are many design approaches for the vector-current control, which is illustrated in Fig. 2.

Vector-current control consists of inner and outer control loops [5] [6]. Fig. 2 shows that the outer control loop feeds the reference currents to the inner control loop in order to maintain an adequate reference voltage for the VSC. Depending on the mode of operation, reference i_d^{ref} is used to control the active power or DC voltage. Similarly, reference i_q^{ref} is used to control the reactive power or AC voltage. There are several ways to calculate the reference currents. In this work, a PI controller with feed-forward is used. For instance, if the active and reactive powers are controlled, the reference currents can be calculated as

$$\mathbf{i}_{dq}^{\text{ref}} = \frac{1}{V}\begin{pmatrix} P^{\text{ref}} + (k_{po} + \frac{k_{io}}{s})(P^{\text{ref}} - P) \\ -Q^{\text{ref}} - (k_{po} + \frac{k_{io}}{s})(Q^{\text{ref}} - Q) \end{pmatrix}, \quad (1)$$

where $V = |\mathbf{v}_{dq}| = \sqrt{v_d^2 + v_q^2}$ is the voltage magnitude at the converter bridge.

Then, the reference currents i_d^{ref} and i_q^{ref} will become input signals for the inner control loop. Inside the inner control loop, the relationship between converter current $\mathbf{i}_{dq} = \begin{pmatrix} i_d & i_q \end{pmatrix}^T$, bridge AC voltage $\mathbf{v}_{dq} = \begin{pmatrix} v_d & v_q \end{pmatrix}^T$, and AC line voltage $\mathbf{u}_{dq} = \begin{pmatrix} u_d & u_q \end{pmatrix}^T$, in dq-plane is

$$\mathbf{v}_{dq} = \mathbf{u}_{dq} + \omega_1 L \begin{pmatrix} i_q \\ -i_d \end{pmatrix} - L\frac{d\mathbf{i}_{dq}}{dt}, \quad (2)$$

where ω_1 is the angular frequency of an AC system, L is the leakage inductance of the transformer. This equation shows that the system is coupled. Thus, a decoupler is added to the inner feedback loop of the system so that a diagonal PI controller can be implemented, which can be expressed as:

$$F_{\text{PI}}(s) = -\begin{pmatrix} k_{pi} + \frac{k_{ii}}{s} & 0 \\ 0 & k_{pi} + \frac{k_{ii}}{s} \end{pmatrix}. \quad (3)$$

Therefore, the ultimate control law for the inner control loop can be formulated as:

$$\mathbf{v}_{dq}^{\text{ref}} = \begin{pmatrix} u_d \\ u_q \end{pmatrix} + F_{\text{PI}}(s)\begin{pmatrix} i_d^{\text{ref}} - i_d \\ i_q^{\text{ref}} - i_q \end{pmatrix} + \omega_1 L \begin{pmatrix} i_q \\ -i_d \end{pmatrix}. \quad (4)$$

III. Test systems

Three test systems, a one-terminal VSC, a point-to-point VSC-HVDC link, and a four-terminal VSC DC grid, were developed to validate the proposed VSC model and its control schemes.

A. One terminal VSC

Figure 1 depicts the one-terminal VSC test system. Its parameters are given in Table I.

TABLE I. Parameters for the one-terminal VSC test system

DC capacitor	$195\mu F$
Reactance of phase reactor	$0.15pu$
Carrier frequency	$1.5kHz$
Nominal apparent power (S_n)	1000 MVA
DC voltage	640 kV
Nominal line voltage (rms)	380 kV
Reactance of transformer leakage inductance	0.18 pu
AC source voltage (line to line)	380 kV
AC source three-phase short circuit level at base voltage	10000 MVA
AC source X/R ratio	10

The PI controllers in both outer and inner control loops were tuned to obtain the desired responses. The tuning method and tests can be found in [3]. The tuned parameters of PI controllers for one-terminal VSC test system are shown in Table II.

TABLE II. PI CONTROLLER PARAMETERS FOR THE ONE-TERMINAL VSC TEST SYSTEM

Parameters	k_{io}	k_{po}	k_{ii}	k_{pi}
Values	1.18	3.02	16.6	0.1533

B. Point-to-point VSC-HVDC link

Figure 3 shows the point-to-point VSC-HVDC link test system, where two one-terminal VSC models are connected by a 750 km-long DC cable. This cable's parameters are shown in Table III.

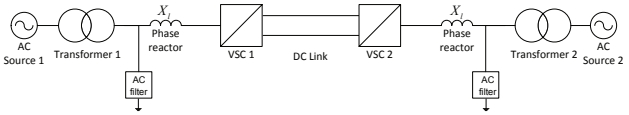

Fig. 3. Circuit diagram of the point-to-point VSC HVDC link

TABLE III. DC CABLE'S PARAMETERS FOR THE POINT-TO-POINT VSC-HVDC LINK TEST SYSTEM

Parameters	Values per km
Line inductance	1.5900×10^{-7}
Line capacitance	2.300×10^{-7}
Line resistance	1.300×10^{-3}

In a point-to-point VSC-VHDC link, one terminal behaves as a rectifier and the other as an inverter. Its bi-directional power flow can be regulated by the outer control loop as presented in Subsection II-B. Although both DC voltage control and active power control belong to the d-axis control mode, note that only one DC voltage control is allowed in each DC grid. Thus, either rectifier or inverter can be chosen for DC voltage control and the other one has to be with active power control. With respect to the q-axis control mode, it is free for both rectifier and inverter to choose either AC voltage control or reactive power control. Inside the rectifier and inverter, same converter parameters shown in Table I were used and the tuned parameters for PI controllers are shown in Table IV.

TABLE IV. PI CONTROLLER PARAMETERS FOR THE POINT-TO-POINT VSC-VHDC LINK TEST SYSTEM

Parameters	k_{io}	k_{po}	k_{ii}	k_{pi}
Values	1.18	3.02	8.3	0.0767

C. Four-terminal VSC DC grid

In the four-terminal VSC DC grid, four VSCs are connected together with a configuration shown in Fig. 4.

The same parameters of converter and DC cables for the point-to-point VSC-VHDC link were used here. However, instead of using constant DC voltage control or active power control, DC voltage droop control was applied. This control scheme is commonly used in multi-terminal DC grids to provide a linear change on the DC voltage as the active power reference changes [3]. Figure 5 shows the characteristics of a DC voltage droop controller, which can be modeled by

$$(V_{dc}^{ref0} - V_{dc}^{ref1}) \times K_{droop} = P_{dc}^{ref1} - P_{dc}^{ref0} \qquad (5)$$

The corresponding controller parameters are shown in Table V.

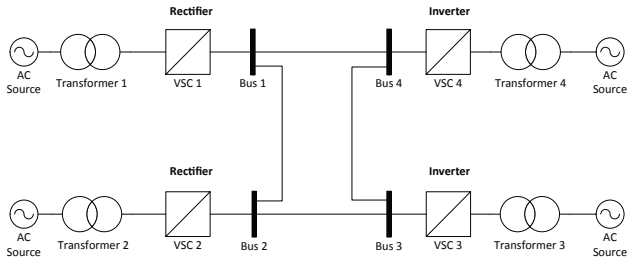

Fig. 4. Configuration of the four-terminal VSC DC grid

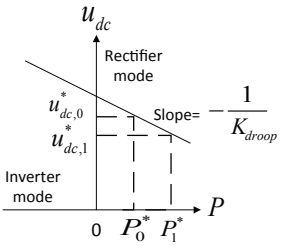

Fig. 5. Characteristics of a DC voltage droop controller

TABLE V. PI CONTROLLER PARAMETERS FOR THE FOUR-TERMINAL VSC DC GRID TEST SYSTEM

Parameters	K_{droop}(inverter1)	K_{droop}(inverter2)	k_{ii}	k_{pi}
Values	0.1	0.1	16.6	0.1533

IV. SIMULATION MODELS AND EXPERIMENTAL VALIDATION PLATFORM

These three test systems were implemented into different simulation tools and a hardware-based emulation platform to validate the proposed VSC model and its control schemes. `Matlab/Simulink` was firstly used to carry out off-line simulation; then, real-time simulation using `Opal-RT`'s real-time simulator was performed; finally, three of the test systems were slightly modified to adapt to the experimental platform due to its power and voltage rating limitations, on which experimental tests were performed.

A. *Matlab/Simulink off-line simulation models*

`Matlab/Simulink` was utilized for off-line simulation. Due to space limitations, only one screenshot of a test system implementation is shown in Fig. 6.

B. Real-time simulation

`Opal-RT` real-time simulators enable to run simulation in real-time, i.e. $1s$ in simulation equals to $1s$ in real life. The goal of implementing models into the real-time simulator is two-fold: (i) to perform fast simulation of the models, and (ii) to exploit the models in hardware-in-the-loop tests with external VSC controls in the future.

To implement a test system into `RT-LAB`, which is the user interface software of `Opal-RT` real-time simulators, the entire system has to be re-arranged into three subsystems referred to as master, slave, and console subsystems [3]. Both the master and slave subsystems can contain computational elements of the model, mathematical operation blocks, input-output blocks, signal generator, etc.; while the console subsystem contains, as

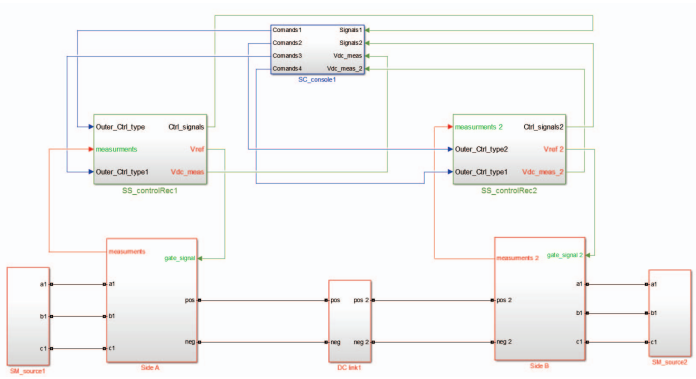

Fig. 6. Graphical implementation of the point-to-point VSC-HVDC link test system in Matlab/Simulink [2]

its names implies, various console components, such as voltage meters, current meters, etc. One screenshot of a test system implementation is shown in Fig. 7.

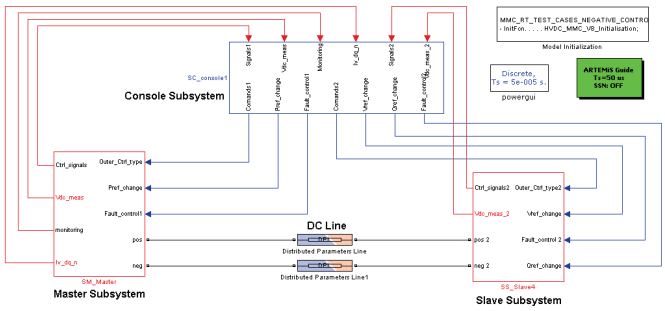

Fig. 7. Graphical implementation of the point-to-point VSC-HVDC link test system in RT-LAB [3]

C. Experimental platform designed and built by CITCEA-UPC for validation

An experimental platform had been designed and built up by CITCEA-UPC for multi-terminal VSC-HVDC transmission system study [7]. The developed setup emulates the behavior of a real HVDC system. The system consists of four VSC converters connected in the DC side by means of a DC grid. A wind farm is emulated using a squirrel cage induction motor which is mechanically coupled to a squirrel cage induction generator which is connected to the wind farm VSC. A photograph and a scheme of the system are shown in Fig. 8 and 9, respectively.

The VSC power converter used in the experimental platform is a two level converter based on IGBTs. The whole device is composed by three boards: the power board, the drivers board and the control board. The control board is based on a Texas Instruments Digital Signal Processor (DSP) TMS320F2808. The DSP interacts with the IGBTs by means of a driver board that provides the necessary gate-excitation signals and also introduces the dead-time. In addition, the drivers board has analogue-based protections, that disconnect the power converter in case of over-current, over-temperature, over-voltage or drivers error. Each grid side power converter is

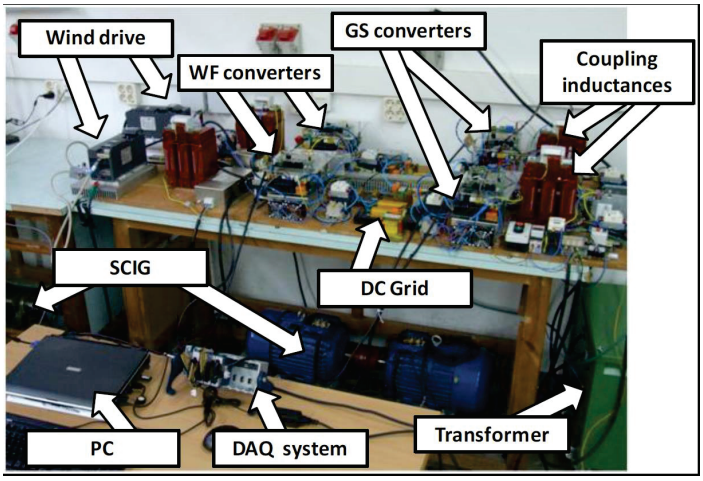

Fig. 8. Photograph of the experimental platform [7]

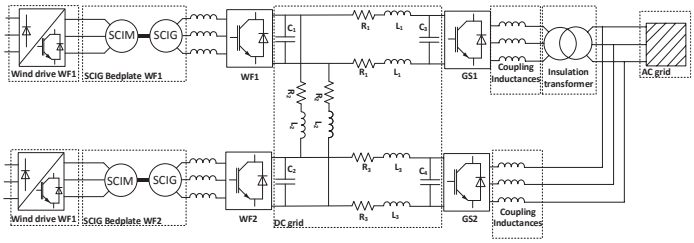

Fig. 9. Scheme of the experimental platform [7]

connected to the AC grid by means of an inductance. Nominal values of the system can be seen in Table VI.

TABLE VI. EXPERIMENTAL PLATFORM PARAMETERS

Parameters	Values
Nominal DC voltage	800 V
Nominal AC current	15 A
Maximum switching frequency	$20kHz$
Coupling inductance	$4.6mH$
Coupling resistance	$0.5omega$

In order to test and verify the proposed generic VSC model and its control schemes, this platform accommodated the different configurations and specifications of the three test systems.

V. RESULTS AND ANALYSIS

For the one-terminal VSC test system, a comparison between simulation results and emulation results in steady state are shown in Fig. 10. As we can see, they have a perfect match.

For the point-to-point VSC-HVDC link test system, Fig. 11 shows the active power and the DC voltage during an active power reference change at GSC2 (the inverter). The power was changed from 0.2 to 1 $p.u.$. From the active power point of view the system was evolving as a first order system with a time constant of 60 ms. The DC voltage at GSC1 (the rectifier) suffered a very small perturbation and the DC voltage at GSC2 (the inverter) changed the steady state equilibrium point due to the increase of the exchanged active power. Simulation and emulation results match well.

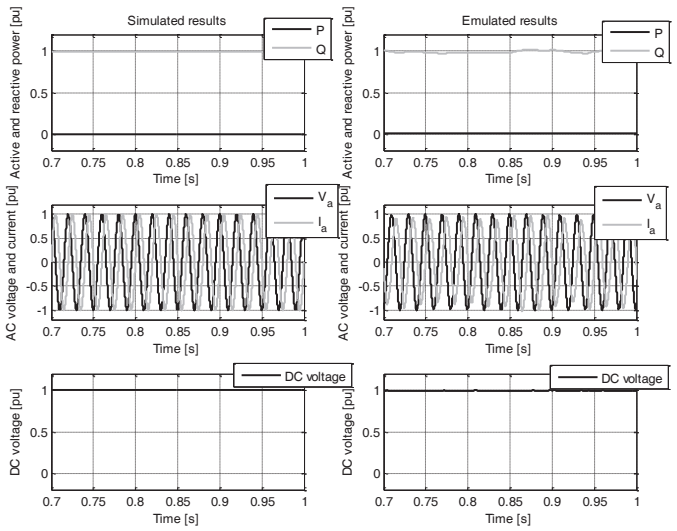

Fig. 10. Comparison between simulation and emulation results of the one-terminal VSC test system in steady state.

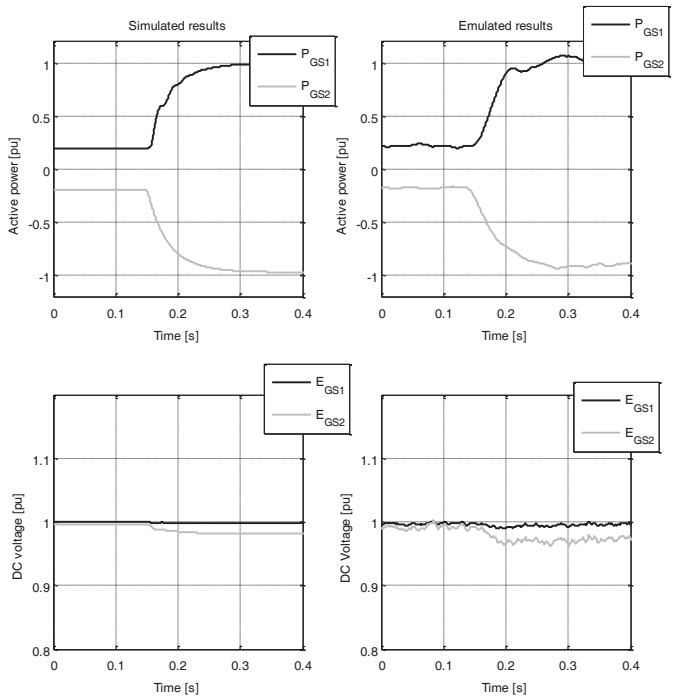

Fig. 11. Comparison between simulation and emulation results of the point-to-point VSC-HVDC link test system during an active power reference change.

A power converter disconnection scenario was applied on the four-terminal VSC DC grid. GS1, one of the inverters shown in Fig. 9, was disconnected at $t = 0.9\ s$. Fig. 12 shows the DC currents and voltages. Once the GS1 was disconnected, the voltage of the DC grid increased by the droop control of GS2. As the droop control was not saturated no power reduction methods were needed. Note that currents of WF1 and WF2 suffered a small decrease due to the voltage increase. In addition, the DC grid voltage reached a new nominal operational point of 1.045 $p.u.$ at time instant of 1.05 s. Simulations show the same performance as the emulations.

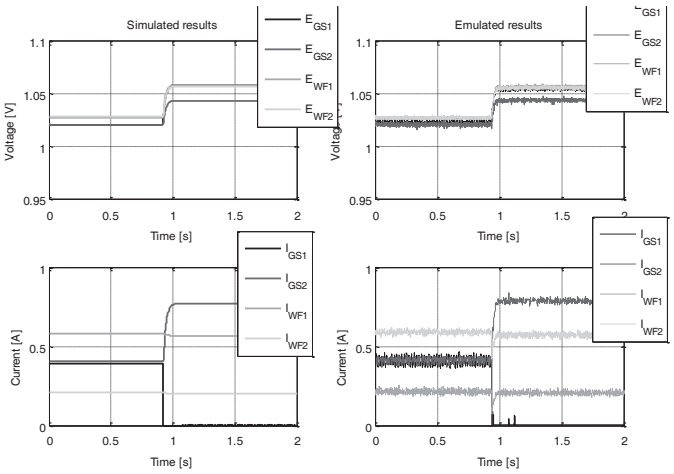

Fig. 12. Comparison between simulation and emulation results of the four-terminal VSC DC grid test system during a disconnection of GS1.

VI. Conclusion

This paper briefly presents partial outcomes of the KIC InnoEnergy project: Generic DC grid off-line and real-time simulation models and tools (Action 2.1 Subtask 2.1.1). A generic VSC model and its control systems are introduced. Three different test systems were developed and implemented in `Matlab/Simulink` for off-line simulations, in `RT-LAB` for real-time simulations, and in the experimental platform for emulations. Due to space limitations, only a few simulation and emulation results are shown in this paper. Nevertheless, these results have illustrated that the control schemes perform satisfactorily during different perturbations. In addition, consistent performances between simulation and emulation results validate the validity and applicability of the proposed generic VSC model. Therefore, they can be freely and widely applied for academic studies and research.

References

[1] L. Zhang, "Modeling and control of VSC-HVDC links connected to weak ac systems, Ph.D. dissertation, KTH, Electrical Machines and Power Electronics, 2010.

[2] L. Vanfretti, N. A. Khan, W. Li, M. R. Kasan, and A. Haider, "Generic VSC and Low Level Switching Control Models for Offline Simulation of VSC-HVDC Systems", *Electric Power Quality and Supply Reliability*, June, 2014.

[3] M. R. Hasan, L. Vanfretti, and W. Li, "Generic High Level VSC-HVDC Grid Controls and Test Systems for Offline and Real Time Simulation", *Electric Power Quality and Supply Reliability*, Jun., 2014.

[4] T. W. Shire, "VSC-HVDC based Network Reinforcement," Delft University of Technology, Delft, 2009.

[5] T. M. Haileselassie, "Control, Dynamics and Operation of Multi-terminal VSC-HVDC Transmission Systems", Ph.D. dissertation, Dept. Elect. Pow. Eng., NTNU, Trondheim, Noway, 2012.

[6] R. Rogersten, L. Vanfretti, W. Li, L. Zhang, and P. Mitra, "A Quantitative Method for the Assessment of VSC-HVdc Controller Simulations in EMT Tools", *IEEE ISGT Europe*, Oct, 2014.

[7] A. Egea-Àlvarez, F. Bianchi, A. Junyent-Ferré, G. Gross, and O. Gomis-Bellmunt, "Voltage Control of Multiterminal VSC-HVDC Transmission System for Offshore Wind Power Plants: Design and Implementation in a Scaled Platform", *IEEE Trans. Industrial Elect.*, vol. 60, no. 6, pp. 23812391, Jun. 2013.